Activity and segregation behavior of $Pd_{75\%}Ag_{25\%}(1\,1\,1)$ during CO oxidation – An in situ NAP-XPS investigation

Ingeborg-Helene Svenum [a,b], Marie D. Strømsheim [c], Jan Knudsen [d,e], Hilde J. Venvik [b,*]

[a] SINTEF Industry, P.O. Box 4760 Torgarden, NO-7465 Trondheim, Norway
[b] Department of Chemical Engineering, Norwegian University of Science and Technology (NTNU), NO-7491 Trondheim, Norway
[c] Hydrogen Mem-Tech, Leirfossvegen 27, NO-7038 Trondheim, Norway
[d] Division of Synchrotron Radiation Research, Department of Physics, Lund University, P.O. Box 118, SE-221 00 Lund, Sweden
[e] MAX IV Laboratory, Lund University, P.O Box 118, SE-221 00 Lund, Sweden

ARTICLE INFO

ABSTRACT

The surface reactivity during CO oxidation over Pd(1 1 1) and $Pd_{75\%}Ag_{25\%}(1\,1\,1)$ single crystals has been investigated using near ambient pressure X-ray photoelectron spectroscopy (NAP-XPS) under excess oxygen conditions (p ≈ 2 mbar, O_2:CO=10). The ($\sqrt{6}\times\sqrt{6}$) Pd_5O_4 surface oxide is present on Pd(1 1 1) when the surface is highly active under the applied conditions. The CO_2 formation profile follows a hysteresis upon temperature cycling between 150 and 450 °C that depends on the temperature ramp rate. The behavior is different for $Pd_{75\%}Ag_{25\%}(1\,1\,1)$, with the CO_2 formation rate considerably lower, no surface oxide and only chemisorbed oxygen present at the surface at high temperature, reversible scrambling of the (near) surface Pd/(Pd+Ag) ratio, and no hysteresis behavior observed. The results suggest that the reactant activation is affected by both surface composition and surface termination, i.e. mechanistically different on $Pd_{75\%}Ag_{25\%}(1\,1\,1)$ than Pd(1 1 1), and less efficient on (1 1 1) as compared to the (1 0 0) alloy counterpart.

1. Introduction

The segregation dynamics in the near-surface region (a few atomic layers) of bimetallic catalysts in response to the chemical environment is important to the catalytic performance. Near-ambient pressure X-ray photoelectron spectroscopy (NAP-XPS) using tuneable, high brilliance, synchrotron light offers the opportunity to determine such segregation and its impact on the surface reaction. We have previously studied the oxidation of CO under excess oxygen over $Pd_{75\%}Ag_{25\%}(1\,0\,0)$ at temperatures up to 600 °C and compared it to pure Pd(1 0 0) [1,2]. Several in situ NAP-XPS and surface X-ray diffraction (SXRD) studies have shown the latter to be terminated by an ordered ($\sqrt{5}\times\sqrt{5}$)R27° surface oxide at high catalytic activity under excess oxygen [2–6], i.e. after light-off and lifting of the inhibiting CO coverage above ~190 °C temperature. In this regime, the reaction rate is usually restricted by the diffusion of CO towards the surface (mass transfer limit – MTL) for the reaction cells adapted to single crystals and XPS [7–9]. Moreover, the extinction, i.e. establishing a high, inhibiting CO coverage upon reducing the temperature, often takes place at a

lower temperature than the ignition [2,10]. But while $Pd_{75\%}Ag_{25\%}(1\,0\,0)$ may form a similar oxide in pure O_2, the oxide is not present in equivalent CO oxidation experiments [1,2]. We also found that $Pd_{75\%}Ag_{25\%}(1\,0\,0)$ exhibited a "reversed" ignition-extinction hysteresis as compared to that of pure Pd(1 0 0). This behaviour was first attributed, based on computational simulations, to originate from segregation of Ag to the surface at high temperature and low coverage [2], and recently we confirmed the presence of a reversible variation in Pd/(Pd+Ag) within the ~6 uppermost atomic layers during temperature cycling under O_2:CO=10 by NAP-XPS measurements [1].

Our measurements also demonstrated that in the case of the $Pd_{75\%}Ag_{25\%}(1\,0\,0)$ alloy surface, the hysteresis in CO_2 formation (activity) was dependent on experimental history in terms of maximum temperature and heating rate, i.e., normal, reversed and no hysteresis behaviour were all observed. Given that the segregation could be detected even at ambient temperature, it seems that adsorbate binding is the main controlling phenomenon for the surface termination, but that the changes cannot be fully captured by a $Pd_{5/2}$ peak originating from the total XPS sampling depth.

Similarly to Pd(1 0 0), a surface oxide can form on Pd(1 1 1) [11–17] and Duan and Henkelman [17] have summarized the experimental findings for CO oxidation over Pd(1 1 1) in their combined

---

DFT and kinetic modelling. Two ordered oxide structures are prevalent under oxygen; a p(2 × 2) overlayer and a ($\sqrt{6} \times \sqrt{6}$) Pd_5O_4 surface oxide equivalent to 0.25 and 0.80 monolayer (ML) coverage, respectively [17]. The mentioned authors estimated similar oxygen binding energy gains for the two, hence their relative stability depends on the oxygen partial pressure. The state of the Pd(111) surface during CO oxidation, the nature of the active site (Pd vs Pd-O), and the mechanistic implications of these are still somewhat debated [6,18]. Early NAP-XPS experiments at O_2:CO=10 and 0.3 mbar by Toyoshima et al. [19] reported the Pd_5O_4 surface oxide as present at high CO_2 formation at 300 °C, but gradual transition to PdO and lower activity at 400 °C. Duan and Henkelman also concluded the thin Pd_5O_4 surface oxide to be thermodynamically stable for O_2:CO $\gtrsim$ 1 and T > 300 °C, with the reaction following a Eley-Rideal mechanism.

Comparable CO oxidation experiments on $Pd_{1-x}Ag_x$(111) alloy surfaces are – to the extent of our knowledge – not available in the literature. The addition of Ag to a Pd surface or catalyst generally moderates the reaction rate both in oxidation and hydrogenation, the latter enabling, e.g., higher alkene yields. In Pd-based hydrogen membranes, Ag addition increases the structural stability and decreases cost with negligible negative effect for an optimum ratio of Pd/Ag $\approx$ 3 on H_2 adsorption, dissociation, and bulk transport (in fact, decreased diffusivity is compensated by increased solubility of H atoms) (see e.g. [20] and references therein). We are, however, still investigating the extent to which segregation phenomena affect the performance of low thickness (<10 μm) polycrystalline membranes. It has long been established that Ag termination is energetically favourable in vacuum/inert, while presence of adsorbates promotes Pd termination [21–23]. Hence, the dynamic response to the gaseous reaction environment is a function of the chemical potential in conjunction with the segregation kinetics [24], i.e., temperature, pressure and composition.

In this work the segregation was monitored in situ for a $Pd_{75\%}$-$Ag_{25\%}$(111) single crystal under CO oxidation (O_2:CO=10) temperature cycles in NAP-XPS. The activity and surface characteristics are compared to Pd(111), as well as the corresponding (100) counterparts. In addition, we have – based on previous experience – improved the experimental protocol for the temperature cycling by establishing a reproducible, oxidized surface at high temperature (450 °C) and applying first cooling and then heating ramps.

2. Materials and methods

The NAP-XPS experiments were performed at the MAX IV Laboratory's HIPPIE beamline [25]. Descriptions of the end-station with the ambient pressure cell (AP-cell) and hemispherical electron analyser with differential pumping have been published elsewhere [26]. The AP-cell used as a reactor with the sample installed allows NAP-XPS measurements pressures up to ~30 mbar. A 300 μm differentially pumped aperture and a sample-aperture distance of ~0.6 mm ensure stable pressure on the sample while minimizing the photoelectron attenuation [27]. Details regarding sample heating and gas exposure are also described elsewhere [1].

Pd(111) and $Pd_{75\%}Ag_{25\%}$(111) single crystals, obtained from Surface Preparation Laboratory and Mateck, respectively, were studied under similar conditions and compared. The single crystals were mounted on steel (304 L) plates and fastened by steel (304 L) clips with a K-type thermocouple spot-welded to the side of the crystal. Cleaning was performed by standard cycles of argon sputtering and subsequent annealing (450–540 °C) in oxygen (p_{O2} ~1·10⁻⁷ mbar). Survey scans were obtained to assess the cleanliness of the crystal, with no additional elements besides Pd and Ag observed except trace amounts of Si on the $Pd_{75\%}Ag_{25\%}$(111) sample that we concluded not to affect the experiments (see Supporting information Fig. S1). The following core level regions were acquired: O 1 s at 650 eV photon energy, Pd and Ag 3d at 450 eV, and C 1s at 450 eV and 390 eV. The same photon energies were applied in our work on $Pd_{75\%}Ag_{25\%}$(100) and represent a compromise between surface sensitivity, scattering cross section, and monochromator performance. All spectra were measured at normal emission and calibrated to the Fermi edge.

CO oxidation over Pd(111) and $Pd_{75\%}Ag_{25\%}$(111) at ~2 mbar during temperature cycling in the range 150–450 °C was investigated following the Ag, Pd and C core levels. The protocol for each CO oxidation cycle was: i) Initial exposure in O_2 (5 mL/min, 1–2 mbar) at 450 °C for ~10 min; ii) addition of CO (0.5 mL/min and total pressure of ~2 mbar) while keeping the sample at 450 °C for ~10 min; iii) cooling to 150 °C; iv) dwell at 150 °C typically around 5 min; and v) heating to 450 °C. Three different temperature ramp rates were applied; 0.1, 0.4 and 1 °C/s. This protocol intended to ensure a relatively stable starting point – an oxidized, Pd-rich surface – between cycles, since red/ox phenomena may take place with CO present and since, albeit slow, segregation may also occur at low temperature [1]. A filter was used on the CO gas line to ensure removal of possible carbonyl species. Quadrupole mass spectrometry (QMS) was used to measure the composition of the gas leaving through the nozzle of the analyser cone, i.e., close to the sample surface. XPS spectra, QMS signals and temperature were recorded separately and subsequently time-correlated and plotted against temperature. Analysis of the acquired core level spectra was performed similar to that of our previous study on $Pd_{75\%}Ag_{25\%}$(100) [1]. The spectra were fitted using a Doniach-Šunjić line shape [28] convoluted with a Gaussian line shape. A linear background was applied. The bulk components of Pd(111) and $Pd_{75\%}Ag_{25\%}$(111) were fitted with an asymmetric line shape, whereas no asymmetry was applied to adsorbate induced peaks of Pd $3d_{5/2}$. All displayed spectra are normalized at the low binding energy side. The areas of the acquired core levels were corrected with cross sections [29] and electron mean free paths of 4.05 and 4.13 Å (Ag 3d), 3.86 and 4.13 Å (Pd 3d), and 0.35 and 8.95 Å (C 1s), respectively. No corrections for differences in transmission through the analyser were made. Full CO oxidation cycles (steps i-v) for Pd(111) and $Pd_{75\%}Ag_{25\%}$(111) showing the CO and CO_2 QMS signals in addition to the temperature profile is shown in Fig. S2.

3. Results

CO_2 formation profiles and overall changes to the core level spectra for Pd(111) (Pd $3d_{5/2}$ and C 1s) and $Pd_{75\%}Ag_{25\%}$(111) (Pd $3d_{5/2}$, Ag $3d_{5/2}$ and C 1s) as acquired in situ during first oxygen exposure and then CO oxidation cycled down to 150 °C and back up to 450 °C are shown in Fig. 1. Fitted Pd $3d_{5/2}$ spectra at selected conditions are plotted in Fig. 2.

Fig. 1a compares the CO_2-MS signals for the two surfaces. Pd (111) displays the characteristic extinction-ignition behavior attributable to mass transfer limitations at high temperature and CO inhibition at low temperature. In excess oxygen, the extinction occurs at ~210 °C (evaluated at 50 %) and the light off appears at ~230 °C with abrupt transitions between the high CO_2 formation regime and CO poisoning. This is commonly observed for Pt-group metals [10,30]. The current results show that the hysteresis behaviour of Pd(111) is dependent of the temperature ramp rate (Fig. S3 a–c), since with slow heating or cooling, the transition between high CO coverage and surface oxide occurs at similar temperature, the surface coverages thus being more equilibrated.

The CO oxidation activity is significantly reduced for the the $Pd_{75\%}Ag_{25\%}$(111) counterpart, to the extent that a mass transfer limit is never reached and with no apparent extinction-ignition
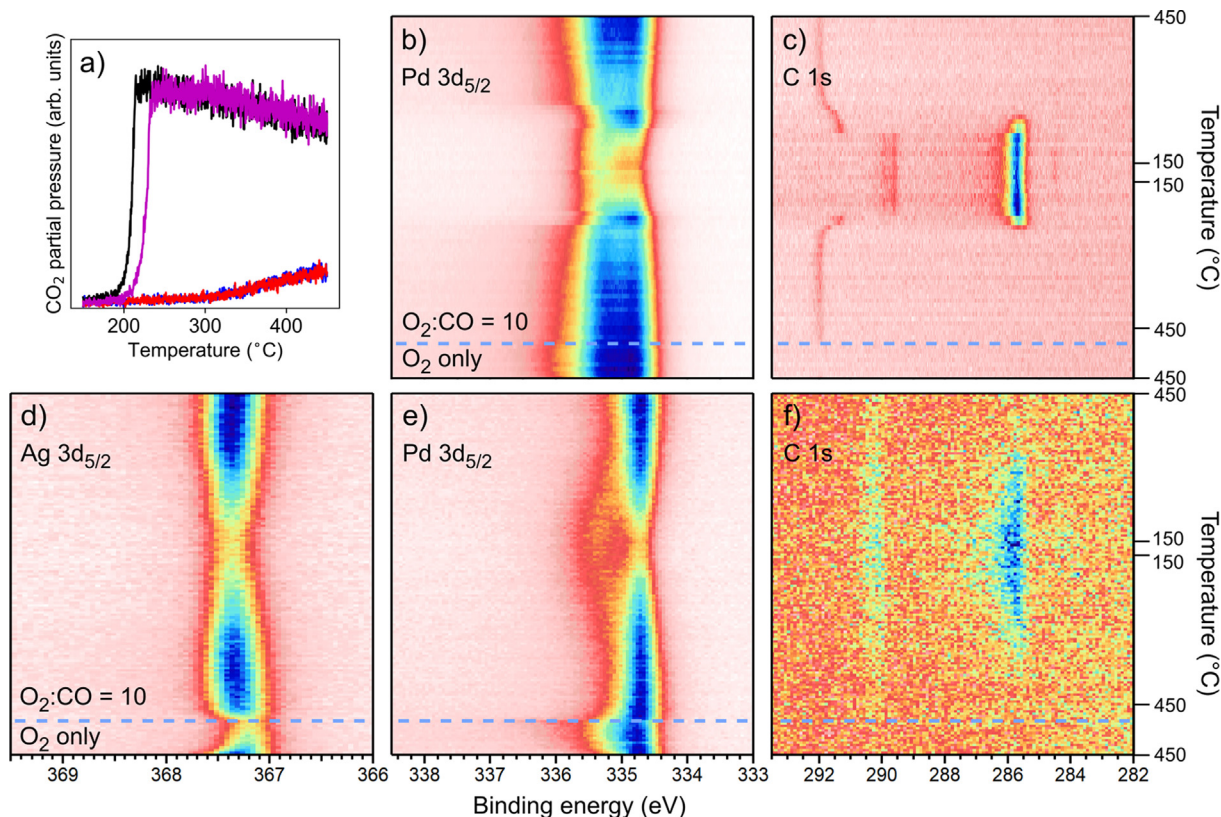
Fig. 1. CO_2 formation profiles and corresponding XPS live spectra (450 eV photon energy) under CO oxidation conditions (O_2:CO=10 at ~2 mbar). The surfaces were initially exposed to O_2 only at 450 °C before introduction of CO (marked with horizontal lines) and cycling from 450 to 150 and back to 450 °C. a) CO_2-MS for Pd(111) in black/magenta and $Pd_{75\%}Ag_{25\%}$(111) in blue/red for cooling/heating (0.4 °C/s), respectively. b) Pd $3d_{5/2}$ and c) C 1s core level regions (0.1 °C/s) for Pd(111). d) Ag $3d_{5/2}$, e) Pd $3d_{5/2}$ and f) C 1s core level regions (0.1 °C/s) for $Pd_{75\%}Ag_{25\%}$(111). The color scale goes from white/pink through red, orange, yellow, green and turquoise to blue/black, with yellow-green in the center of the intensity scale. (For interpretation of the references to color in this figure legend, the reader is referred to the web version of this article.)
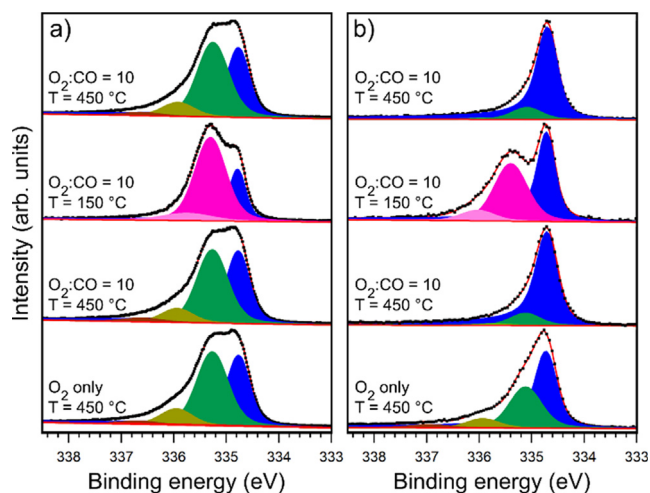
Fig. 2. Fitted Pd $3d_{5/2}$ spectra for (a) Pd(111) and (b) $Pd_{75\%}Ag_{25\%}$(111) from Fig. 1 taken at 450 °C with O_2 only, and at 450–150–450 °C for temperature cycling under CO oxidation conditions (O_2:CO=10 at ~2 mbar, 0.1 °C/s). Bulk components are represented in blue, oxygen induced components are represented in green and brown and CO induced compoents are represented in pink and light pink. (For interpretation of the references to color in this figure legend, the reader is referred to the web version of this article.)

hysteresis behaviour (Fig. S3d–f). The decrease/increase in CO_2 formation with temperature is slow, and there appears to exist two regimes, 300–400 °C and 200–300 °C, of which the latter represents very low activity. These reactivity profiles were consistent

over repeated cycles, irrespective of the temperature ramp rate. This indicates that the chosen protocol enables linking the behaviour to the surface composition of the bimetallic system without taking into account the temperature cycling and reactant exposure history of the $Pd_{75\%}Ag_{25\%}$(111) alloy surface.

The Pd $3d_{5/2}$ spectrum of Pd(111) (Fig. 1b) shows overall little change upon introducing CO alongside oxygen and ramping down in temperature until the point at which the activity drops. The extinction at ~210 °C is associated with the appearance of adsorbed CO (285.7 eV) in the C 1s core level spectra (Fig. 1c), signifying high CO coverage. The main C 1s component at 285.7 eV corresponds to CO occupying bridge and hollow sites on the Pd (111) surface, as previously found (285.6 eV) for 0.5 ML CO [31]. In addition, the peak assigned to gas phase CO_2 (~292.0 eV) disappears while that of gas phase CO (~289.7 eV) appears [3]. The temperature dependence is similar upon cooling and heating, with the exception of the (rate dependent) difference in transition temperature. The transition in and out of the CO inhibited regime is associated with a shift in the sample work function – seen as a shift in the CO_2 gas phase contribution [32–34].

The changes throughout the cycle are more prominent for the $Pd_{75\%}Ag_{25\%}$(111) surface (Fig. 1d–f). During the short initial oxidation under only O_2 exposure at 450 °C, the Ag $3d_{5/2}$ signal clearly weakens and the total Pd $3d_{5/2}$ contribution increases. This shows that Pd segregates to the surface at these conditions. There is a clear change upon adding CO to start the reaction, with Ag $3d_{5/2}$ again increasing and the high binding energy part of the Pd $3d_{5/2}$ contribution diminishing. When decreasing and thereafter increasing the temperature there are no abrupt transitions, and the cooling and heating behaviours are similar. Pd $3d_{5/2}$ develops a small

high binding energy contribution. The weak C 1s contributions are consistent with gradual build-up of adsorbed CO (285.7 eV). The presence of gas phase CO ($\sim$290.3 eV) near the surface suggests absence of mass transfer limitations, but its varying intensity over the temperature cycle is mainly caused by temperature effects, such as thermal expansion affecting the gas volume probed. The difference of 0.6 eV between gas phase CO on the two surfaces is due to changes in work function between Pd(111) and $Pd_{75\%}$-$Ag_{25\%}$(111). Christmann and Ertl [35] reported a difference in work function of about 0.6 eV between Pd and Pd-Ag (22 % Ag) films at room temperature with adsorbed CO.

The details of the Pd $3d_{5/2}$ spectra are better discussed in terms of high-resolution spectra as displayed in Fig. 2. Formation of a Pd surface oxide results from the initial exposure to O_2 at 450 °C on both Pd(111) and $Pd_{75}Ag_{25}$(111) (Fig. 2a-b, lower panels). The Pd $3d_{5/2}$ spectra contain two significant oxygen induced components in addition to the bulk component (in blue), which can be fitted at 334.7 eV for both samples [1,15,36]. For Pd(111) (Fig. 2a), the oxide peaks are large relative to the bulk peak and shifted by 0.4 and 1.2 eV (in green and mustard), consistent with the Pd_4O_5 surface oxide with twofold and fourfold coordinated Pd atoms previously reported [11,37]. This assignment is corroborated by the ratio between the two oxygen induced peaks, which is 1:0.22, i.e., same as previously reported in the literature [11]. In addition, a minor peak at 336.9 eV is included to the fit, indicating that a small fraction of multilayer Pd-O has formed on the Pd(111) surface [12,15,38]. Transition from an oxidized surface to CO oxidation conditions introduces practically no changes to the spectrum of Pd(111). Hence, the predominant surface structure when the surface is highly active, under the conditions applied here, is the $(\sqrt{6}\times\sqrt{6})$ Pd_5O_4 surface oxide. The CO inhibited regime at low temperature is associated with a major contribution in Pd $3d_{5/2}$ (335.4 eV, in pink) due to adsorbed CO in 3-fold hollow sites and bridge sites [15,31], and a weak contribution from CO in top sites (336.0 eV, in light pink) [15].

The $Pd_{75\%}Ag_{25\%}$(111) surface exhibits similar features as Pd (111) under pure oxygen exposure (Fig. 2b, lower panel). The two surface oxide induced Pd $3d_{5/2}$ peaks are again shifted by 0.4 and 1.2 eV (in green and mustard) with an intensity ratio of 1:0.22. The total intensity of the two oxygen induced peaks is considerably lower relative to that of the Pd 3d bulk component than was the case for Pd(111). This implies presence of the same surface oxide as Pd(111), but without completely covering the surface. Then, contrarily to the pure Pd(111) surface [15] but similar to $Pd_{75\%}Ag_{25\%}$(100) [2], the peaks representative of a surface oxide immediately disappear upon introducing CO albeit the high O_2 excess (10:1). Only a small contribution ascribed to chemisorbed oxygen remains, as also inferred for $Pd_{75\%}Ag_{25\%}$(100) [2]. As the temperature is decreased to 150 °C, two CO induced contributions appear in the Pd $3d_{5/2}$ spectrum, at binding energies of 335.4 eV (3-fold hollow and bridge, in pink) and 336.0 eV (top, in light pink), respectively, as for Pd(111). The corresponding Ag $3d_{5/2}$ spectra are shown in Fig. S4 and have one contribution at around 367.3 eV, similar to that of the Ag $3d_{5/2}$ bulk component found for $Pd_{75\%}Ag_{25\%}$(100) [1]. As for Pd(111), the spectrum acquired at the end of the CO oxidation cycle at 450 °C (Fig. 2b, top panel) shows no significant difference from that obtained initially (Fig 2b, second panel from the bottom).

Fig. 3 shows the relative amount of Pd in comparison to the total amount of Pd and Ag in the uppermost atomic layers of $Pd_{75\%}$-$Ag_{25\%}$(111) for the CO oxidation series with heating rates of 0.1, 0.4 and 1 °C/s. Each point in the graphs is based on peak areas from a single sweep of the Pd $3d_{5/2}$ and Ag $3d_{5/2}$ core levels (as shown in Fig. 1d and e for the 0.1 °C/s case). During the initial oxidation at 450 °C, the surface becomes enriched in Pd as the Pd surface oxide establishes. The segregation behaviour of the $Pd_{75\%}Ag_{25\%}$(111) sur-
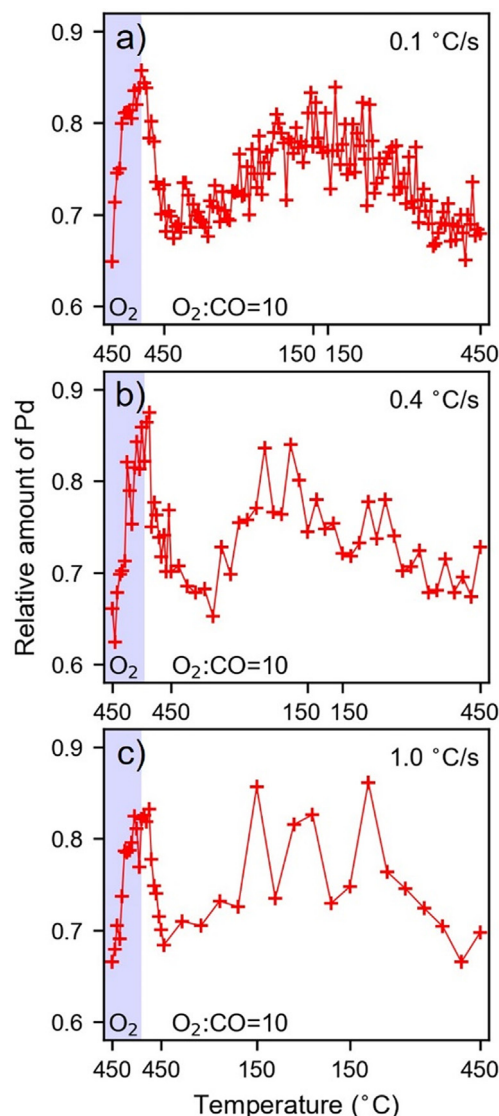
Fig. 3. The relative amount of Pd (Pd/(Pd+Ag)) in $Pd_{75\%}Ag_{25\%}$(111) throughout the initial oxidation (indicated by shade) and temperature cycling from 450 to 150 to 450 °C under CO oxidation conditions (O_2:CO=10 at $\sim$2 mbar) at a rate of (a) 0.1 °C/s, (b) 0.4 °C/s and (c) 1 °C/s.

face is fairly reproducible under these conditions, reaching a relative amount of Pd near the surface of about 0.85 after $\sim$10 min oxidation. Upon introducing CO at 450 °C, the relative amount of Pd decreases by 20–25 % as the oxide is lifted. During the oxidation series with a temperature ramp of 0.1 °C (Fig. 3a), the fraction of Pd again increases, from $\sim$0.7 to $\sim$0.8, as the temperature decreases to 150 °C. This behaviour is reversed upon increasing the temperature back to 450 °C. The temperature ramp rate of 0.4 °C/s is less resolved but displays a similar profile (Fig. 3b). At 1 °C/s (Fig. 3c), however, the temperature ramp rate is too fast to capture all the details of the segregation.

The surface sensitivity of the Pd ratio assessment is limited to a few layers [1]. Thus, since CO adsorbs preferentially to Pd sites in Pd-Ag alloy surfaces [39–44], monitoring the relative amount of Pd bound to CO adsorbed on the surface provides additional information on the composition of the topmost surface layer. The peak areas representative of Pd bound to CO relative to that of total metal (Pd $3d_{5/2}$ + Ag $3d_{5/2}$) of $Pd_{75\%}Ag_{25\%}$(111) for the three CO oxidation series with the different temperature ramp rates are shown in Fig. 4. At around 300 °C, CO starts to accumulate on the surface
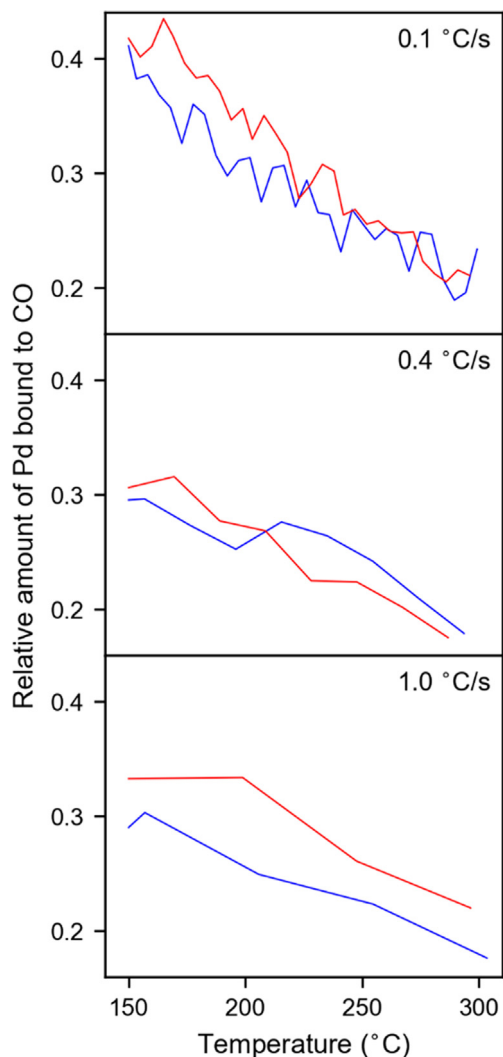
Fig. 4. The relative amount of Pd bound to CO to the total amount of Pd and Ag in Pd$_{75\%}$Ag$_{25\%}$(1 1 1) in the range 150 to 300 °C, during temperature cycling from 450 to 150 to 450 °C under CO oxidation conditions (O$_2$:CO=10 at ∼2 mbar) at a rate of (a) 0.1 °C/s, (b) 0.4 °C/s and (c) 1 °C/s. The blue/red curves indicate cooling/heating, respectively. (For interpretation of the references to color in this figure legend, the reader is referred to the web version of this article.)

(higher temperatures therefore not included to the plot), as also seen from the C 1s spectrum in Fig. 1f. Decreasing the temperature further leads to increased CO coverage on the surface, with the relative amount reaching 0.4 at 150 °C for the 0.1 °C/s series (Fig. 4a). Lower relative amounts of CO are obtained for the two series with faster temperature ramp rates, about 0.3, but with limited experimental precision. The corresponding ratio for Pd(1 1 1) at 150 °C is 0.7, for which a coverage in slight excess of 0.5 ML [18,45,46] may be assumed, since there is a minor contribution from CO in top sites. The ratio between the CO induced contribution in the Pd 3d and C 1s spectrum amounts to about 2:1 for both Pd(1 1 1) and Pd$_{75\%}$Ag$_{25\%}$(1 1 1).

The C 1s spectrum confirms the trends outlined above and the spectra for Pd$_{75\%}$Ag$_{25\%}$(1 1 1) and Pd(1 1 1) are compared in Fig. S5. The main peak attributable to CO occurs at similar binding energy for the two systems. The difference in sample composition yields a difference in the work function, noticeable as a shift in the CO gas phase contribution. The difference in CO coverage is confirmed (0.1 °C/s series), with the peak area ratios C/(C+Pd+Ag) amounting to 0.28 and 0.17 for Pd(1 1 1) and Pd$_{75\%}$Ag$_{25\%}$(1 1 1),

respectively. This implies that the CO coverage is reduced by about 40 %. Hence, a significant fraction of Ag, likely around 40 % [43] is present in the topmost surface layer for Pd$_{75\%}$Ag$_{25\%}$(1 1 1) at 150 °C.

4. Discussion

These results confirm adsorbate induced segregation in Pd$_{75\%}$-Ag$_{25\%}$(1 1 1) and that the amount of Pd in the surface depends on CO coverage as previously predicted for a Pd$_3$Ag(1 1 1) model surface [22,23] and shown experimentally for Pd$_{75\%}$Ag$_{25\%}$(1 0 0) [1]. In the following, we discuss the somewhat striking differences between the two surface terminations, and correlate this to the effect of Ag and the characteristics of the Pd surface oxides.

The cooling and heating CO$_2$ formation profiles are similar for all the three different temperature ramp rates investigated, suggesting that the surface segregation dynamics in Pd$_{75\%}$Ag$_{25\%}$(1 1 1) can follow the changes in reaction conditions. This was not quite the case in our study of the corresponding (1 0 0) surface. This we attribute partially or wholly to the experimental protocol, where we have changed from cycling upwards after residing at ambient temperature at varying time and exposure and then down, to starting from a well-defined Pd surface oxide at elevated temperature (450 °C) cycling down and then up. This at least eliminates the impact of slow, but noticeable, segregation at low temperature. Working with (1 0 0), we were also able to explore higher temperatures (up to 600 °C) than in the present work and this had a dramatic effect on the CO$_2$ formation profiles, which change from one temperature cycle to the next. Even in the presence of adsorbates, high temperature promotes Ag termination due to the low sticking [2], and in addition the segregation phenomena may extend further into the bulk as the solid state diffusion is facilitated. Likewise, the variation in Pd/(Pd+Ag) and relative amount of Pd with CO adsorbed (0.3–0.4) between the temperature ramp rates most likely reflect time-limitations in the experimental precision rather than that the surface composition and resulting CO coverage being impacted by segregation kinetics. For the higher ramp rates, the number of experimental points is low, and each spectrum series (∼50 sec) is impacted by temperature change during its acquisition.

The present work establishes, moreover, that during CO oxidation in excess O$_2$, the Pd surface oxide is present on Pd(1 1 1) when it is highly active, as also previously reported [15,17,19]. This is very clear from the observed work function shift alongside the Pd$_4$O$_5$ surface oxide fingerprint in the Pd 3d$_{5/2}$ spectrum. Replacing 25 % of the Pd by Ag changes the active surface to metallic under O$_2$:CO=10, with some chemisorbed O for both terminations. The introduction of Ag impacts, however, the (1 1 1) case much more severely than the (1 0 0) in terms of kinetics. Care must be taken in comparing activity data that are partially affected by mass transfer, which depend on the reaction cell and sample geometry as well as flow, concentrations and pressure. But now we have Pd$_{75\%}$-Ag$_{25\%}$(1 1 1) and (1 0 0) cases [1] that have been obtained at the same end station and reaction cell, and comparable total pressures. In addition, the older work on Pd$_{75\%}$Ag$_{25\%}$(1 0 0) from a different beamline shows qualitatively similar behaviour in comparison to Pd(1 0 0) [2]. In contrast, the activity of Pd$_{75\%}$Ag$_{25\%}$(1 1 1) is (reproducibly with the new protocol) very low and nowhere near any MTL, while the activity of the ($\sqrt{6}\times\sqrt{6}$) Pd$_5$O$_4$ surface oxide terminated Pd(1 1 1) surface is very high.

The analysis based on relative amount of (near) surface Pd and Pd bound to CO as function of temperature does not provide a straightforward answer to the prominent difference in activity between Pd$_{75\%}$Ag$_{25\%}$(1 1 1) and Pd$_{75\%}$Ag$_{25\%}$(1 0 0). If anything, the relative amounts of Pd are slightly lower in the (1 0 0) as compared to the (1 1 1) case for a given temperature [1], while the activity is

higher. The relative amount of adsorbed CO is also larger for $Pd_{75\%}Ag_{25\%}(111)$ compared to $Pd_{75\%}Ag_{25\%}(100)$ at 150 °C, 0.3 vs 0.15 upon decreasing the temperature to 150 °C under similar conditions. Thus, the (111) surface is as least as Pd rich as its (100) counterpart, and we may need to look at the structure and the activation of CO and oxygen.

The higher number of Pd bonded to CO may in part be explained by differences in adsorption sites. On the (100) facet of palladium-based surfaces, CO is known to occupy bride sites at coverages up to 0.5 ML with the surface Pd atoms coordinated to one or two CO molecules [47]. At similar coverage, CO adsorbs in both hollow and bridge sites on (111), for which all the surface Pd atoms are coordinated to CO [15,31]. At higher coverages also top sites can become occupied for both surface orientations. For the Pd-Ag surfaces, the adsorption site can also change depending on available Pd atoms in the surface, since CO only bonds to Pd [39–44]. In Pd-Ag systems, CO is known to bind strongest to hollow sites made up by Pd [23,43], but the availability of such sites is reduced as the amount of Ag in the topmost surface layer increases. This leads to higher amount of bridge and top bonded CO on $Pd_{75\%}Ag_{25\%}(111)$, which is consistent with previous results for a Pd-Ag surface alloy [43]. Even though it was difficult to distinguish hollow and bridge bonded CO in our Pd $3d_{5/2}$ fitting, a higher relative amount of top bonded CO is present in the spectra.

The higher amount of Pd bonded to CO at 150 °C also indicates that CO binds stronger to $Pd_{75\%}Ag_{25\%}(111)$ than to $Pd_{75\%}Ag_{25\%}(100)$. In general, CO adsorbs stronger to hollow sites as compared to bridge sites. The stronger CO binding is also supported by the fact that the onset of CO_2 formation occurs at higher temperature. Previous investigations of CO oxidation comparing Pd(100) and Pd(111) predicted that coverage effects influenced the activity of the latter surface orientation to a larger extent [48]. This may still be valid for the bimetallic system. The higher adsorption energy of CO leads to a higher desorption temperature, and with CO situated in hollow sites three surface Pd atoms are likely inhibited on Pd(111)/$Pd_{75\%}Ag_{25\%}(111)$. The stronger adsorption of CO may hence be one reason for its lower activity towards CO_2 formation for $Pd_{75\%}Ag_{25\%}(111)$ relative to $Pd_{75\%}Ag_{25\%}(100)$.

As the temperature increases beyond ∼300 °C, adsorbed CO is no longer detectable from the $Pd_{75\%}Ag_{25\%}(111)$ spectra (C 1s, Fig. 1f), i.e., the coverage is very low, and the difference in activity between Pd(111) and $Pd_{75\%}Ag_{25\%}(111)$ cannot be ascribed to CO poisoning. Moreover, even though a surface oxide can form on the $Pd_{75\%}Ag_{25\%}(111)$ surface under pure oxygen exposure at 450 °C, it immediately disappears upon introduction of CO, rendering the surface metallic and increasingly Ag rich. The activation of oxygen may hence be less efficient and mechanistically different on $Pd_{75\%}Ag_{25\%}(111)$ as compared to Pd(111). Albeit the small Pd $3d_{5/2}$ contribution ascribed to chemisorbed oxygen, the activation of O_2 is not sufficiently fast to replace the oxygen removed by CO_2 formation on $Pd_{75\%}Ag_{25\%}(111)$. This supports the notion of the Pd_4O_5 surface oxide as key to the high CO oxidation activity over Pd(111) through Mars-van Krevelen (O_2 activation) and/or Eley-Rideal (CO activation) type steps [17,49].

Finally, an advantage of a moderated Pd oxidation catalyst is that it offers a direct link between activity and the detailed surface characteristics, i.e., a measurable rate *and* little or no impact of mass transfer limitations. This has been difficult under the geometrical and analytical restrictions of in situ AP-XPS investigations, requiring a well-defined (single) crystal surface inside a volume that easily lends itself to concentration gradients [50,51]. Oxidations are often so fast that diffusion limitations are quickly established, while the product formation over single crystals can be difficult to quantify in slower systems such as CO/CO_2 hydrogenation when combined with in situ spectroscopy or microscopy [52]. The alloying introduces alternative challenges, though, since the

reaction rate will be impacted by the reactant and temperature-controlled segregation. As the temperature is increased, more Ag segregates to the surface and this supresses activation of oxygen, as well as CO adsorption, and hence CO_2 formation.

Nevertheless, an apparent activation energy was estimated from the 320–400 °C CO_2 formation data as 28 ± 3 kJ/mol with the Arrhenius plot displayed in Fig. S6. We chose this temperature interval due to a reasonable signal to noise ratio and limited Pd/Ag exchange in the near surface region as inferred from Fig. 3 (keeping in mind that the exchange to/from the topmost layer may be more significant). This value may be compared to experimentally determined barriers for CO oxidation over Pd(111) in the range 50–160 kJ/mol that in different ways take into account coverage and (surface) oxide effects and generally yield higher barriers at low coverage and higher temperature [53,55–57]. The Pd/Ag scrambling thus clearly affects the apparent barrier, and a more exact determination would require more precise control of the surface composition across the temperature range, preferentially by increasing the NAP-XPS surface sensitivity. An even lower barrier seemingly exists in the 200–300 °C (∼7 kJ/mol, low S/N), with the activation likely moderated by more prominent changes in the surface Pd/Ag ratio.

5. Conclusion

The present work demonstrates how the surface termination and segregation in a $Pd_{75\%}Ag_{25\%}(111)$ single crystal can be studied in conjunction with the CO oxidation surface reactivity in NAP-XPS. An experimental protocol involving first creating a PdO layer in the near-surface region enabled better reproducibility over repeated temperature cycling, i.e., minimized impact of the exposure and cycling history of the alloy compared to our previous work on $Pd_{75\%}Ag_{25\%}(100)$. The Pd(111) results support previous reports claiming this surface to be terminated by a $(\sqrt{6} \times \sqrt{6})$ Pd_5O_4 surface oxide at high activity, during which the CO_2 formation is mass transfer limited in the present set-up. The transition to/from a CO inhibited Pd(111) surface with no surface oxide upon decreasing/increasing temperature is abrupt with the associated CO_2 formation hysteresis being dependent on the temperature ramp rate.

The C 1s comparison with Pd(111) also rationalized that about 40 % of Ag atoms are present in the $Pd_{75\%}Ag_{25\%}(111)$ surface at 150 °C and O_2:CO=10. This fraction increases with temperature, as shown by the relative amount of Pd in the near-surface region (Pd/(Pd+Ag)) and the relative amount of Pd bound to CO to the total amount of Pd and Ag decreasing. This behavior is reversible, as is the reactivity, and shows that the termination is largely adsorbate coverage controlled. The CO_2 formation is much lower than on Pd(111) and there are no hysteresis effects. In contrast to Pd(111), and albeit the $(\sqrt{6} \times \sqrt{6})$ Pd_5O_4 surface oxide also forming $Pd_{75\%}Ag_{25\%}(111)$ under pure O_2, the surface oxide is immediately lifted upon changing to O_2:CO=10 at 450 °C and only small amounts of chemisorbed O are present on the surface. An activated reaction with gas phase CO present near the surface suggests absence of mass transfer limitations for the Ag moderated Pd system, but the apparent activation energy (∼30 kJ/mol) obtained from the data is probably affected by the temperature dependent surface Pd/Ag ratio as well as coverage effects. As the temperature increases beyond ∼300 °C and the CO coverage becomes low, inefficient activation of O_2 is likely causing the poor activity observed for the (111) metallic alloy surface.

Finally, there are some interesting differences between $Pd_{75\%}Ag_{25\%}(111)$ and its (100) counterpart. The terminations are similar with respect to formation of surface oxides under pure O_2 ($(\sqrt{5} \times \sqrt{5})R27°$ in the case of Pd(100)) that are lifted upon addition of CO. But the presence of 25 % Ag in the alloy affects the $Pd_{75\%}$-

$Ag_{25\%}(111)$ reactivity more severely than $Pd_{75\%}Ag_{25\%}(100)$, although the relative amount of Pd in the near-surface region (Pd/(Pd+Ag)) and the relative amount of Pd bound to CO to the total amount of Pd and Ag both are higher in the former. We suggest that this originates from a stronger binding of CO compared to $Pd_{75\%}Ag_{25\%}(100)$, and also relative to $Pd(111)$.

Data availability

Data will be made available on request.

Declaration of Competing Interest

The authors declare that they have no known competing financial interests or personal relationships that could have appeared to influence the work reported in this paper.

Acknowledgments

Appendix A. Supplementary material

Supplementary data to this article can be found online at https://doi.org/10.1016/j.jcat.2022.11.038.

References

[1] M.D. Strømsheim, I.-H. Svenum, M. Mahmoodinia, V. Boix, J. Knudsen, H.J. Venvik, Segregation dynamics of a Pd-Ag surface during CO oxidation investigated by NAP-XPS, Catal. Today. 384–386 (2022) 265–273, https://doi.org/10.1016/j.cattod.2021.02.007.

[2] V.R. Fernandes, M.V. den Bossche, J. Knudsen, M.H. Farstad, J. Gustafson, H.J. Venvik, H. Grönbeck, A. Borg, Reversed Hysteresis during CO Oxidation over Pd$_{75}$Ag$_{25}$(100), ACS Catal. 6 (2016) 4154–4161, https://doi.org/10.1021/acscatal.6b00658.

[3] S. Blomberg, M.J. Hoffmann, J. Gustafson, N.M. Martin, V.R. Fernandes, A. Borg, Z. Liu, R. Chang, S. Matera, K. Reuter, E. Lundgren, *In situ* X-ray photoelectron spectroscopy of model catalysts: at the edge of the gap, Phys. Rev. Lett. 110 (2013), https://doi.org/10.1103/PhysRevLett.110.117601.

[4] J. Knudsen, T. Gallo, V. Boix, M.D. Strømsheim, G. D'Acunto, C. Goodwin, H. Wallander, S. Zhu, M. Soldemo, P. Lömker, F. Cavalca, M. Scardamaglia, D. Degerman, A. Nilsson, P. Amann, A. Shavorskiy, J. Schnadt, Stroboscopic operando spectroscopy of the dynamics in heterogeneous catalysis by event-averaging, Nat. Commun. 12 (2021) 6117, https://doi.org/10.1038/s41467-021-26372-y.

[5] R. van Rijn, O. Balmes, R. Felici, J. Gustafson, D. Wermeille, R. Westerström, E. Lundgren, J.W.M. Frenken, Comment on "CO Oxidation on Pt-Group Metals from Ultrahigh Vacuum to Near Atmospheric Pressures. 2. Palladium and Platinum", J. Phys. Chem. C. 114 (2010) 6875–6876, https://doi.org/10.1021/jp911406x.

[6] M.A. van Spronsen, J.W.M. Frenken, I.M.N. Groot, Surface science under reaction conditions: CO oxidation on Pt and Pd model catalysts, Chem. Soc. Rev. 46 (2017) 4347–4374, https://doi.org/10.1039/C7CS00045F.

[7] F. Duprat, Light-off curve of catalytic reaction and kinetics, Chem. Eng. Sci. 57 (2002) 901–911, https://doi.org/10.1016/S0009-2509(01)00409-2.

[8] F. Gao, Y. Wang, D.W. Goodman, Reply to "Comment on 'CO Oxidation on Pt-Group Metals from Ultrahigh Vacuum to Near Atmospheric Pressures. 2. Palladium and Platinum, J. Phys. Chem. C. 114 (2010), https://doi.org/10.1021/jp100134e, 6874–6874.

[9] E. Lundgren, C. Zhang, L.R. Merte, M. Shipilin, S. Blomberg, U. Hejral, J. Zhou, J. Zetterberg, J. Gustafson, Novel in situ techniques for studies of model catalysts, Acc. Chem. Res. 50 (2017) 2326–2333, https://doi.org/10.1021/acs.accounts.7b00281.

[10] D. Vogel, C. Spiel, Y. Suchorski, A. Trinchero, R. Schlögl, H. Grönbeck, G. Rupprechter, Local catalytic ignition during CO oxidation on low-index Pt and Pd surfaces: a combined PEEM, MS, and DFT study, Angew. Chem. Int. Ed. 51 (2012) 10041–10044, https://doi.org/10.1002/anie.201204031.

[11] E. Lundgren, G. Kresse, C. Klein, M. Borg, J.N. Andersen, M. De Santis, Y. Gauthier, C. Konvicka, M. Schmid, P. Varga, Two-dimensional oxide on Pd (111), Phys. Rev. Lett. 88 (2002) 246103, https://doi.org/10.1103/PhysRevLett.88.246103.

[12] G. Ketteler, D.F. Ogletree, H. Bluhm, H. Liu, E.L.D. Hebenstreit, M. Salmeron, In situ spectroscopic study of the oxidation and reduction of Pd(111), J. Am. Chem. Soc. 127 (2005) 18269–18273, https://doi.org/10.1021/ja055754v.

[13] N. Kasper, P. Nolte, A. Stierle, Stability of surface and bulk oxides on Pd(111) revisited by in situ X-ray diffraction, J. Phys. Chem. C. 116 (2012) 21459–21464, https://doi.org/10.1021/jp307434g.

[14] J. Klikovits, E. Napetschnig, M. Schmid, N. Seriani, O. Dubay, G. Kresse, P. Varga, Surface oxides on Pd(111): STM and density functional calculations, Phys. Rev. B 76 (2007), https://doi.org/10.1103/PhysRevB.76.045405.

[15] R. Toyoshima, M. Yoshida, Y. Monya, Y. Kousa, K. Suzuki, H. Abe, B.S. Mun, K. Mase, K. Amemiya, H. Kondoh, In situ ambient pressure XPS study of CO oxidation reaction on Pd(111) surfaces, J. Phys. Chem. C. 116 (2012) 18691–18697, https://doi.org/10.1021/jp301636u.

[16] F. Zhang, T. Li, L. Pan, A. Asthagiri, J.F. Weaver, CO oxidation on single and multilayer Pd oxides on Pd(111): mechanistic insights from RAIRS, Catal. Sci. Technol. 4 (2014) 3826–3834, https://doi.org/10.1039/C4CY00938J.

[17] Z. Duan, G. Henkelman, CO oxidation on the Pd(111) surface, ACS Catal. 4 (2014) 3435–3443, https://doi.org/10.1021/cs5006025.

[18] F. Schiller, M. Ilyn, V. Pérez-Dieste, C. Escudero, C. Huck-Iriart, N. Ruiz del Arbol, B. Hagman, L.R. Merte, F. Bertram, M. Shipilin, S. Blomberg, J. Gustafson, E. Lundgren, J.E. Ortega, Catalytic oxidation of carbon monoxide on a curved Pd crystal: spatial variation of active and poisoning phases in stationary conditions, J. Am. Chem. Soc. 140 (2018) 16245–16252, https://doi.org/10.1021/jacs.8b09428.

[19] H. Kondoh, R. Toyoshima, Y. Monya, M. Yoshida, K. Mase, K. Amemiya, B.S. Mun, In situ analysis of catalytically active Pd surfaces for CO oxidation with near ambient pressure XPS, Catal. Today 260 (2016) 14–20, https://doi.org/10.1016/j.cattod.2015.05.016.

[20] N. Vicinanza, I.-H. Svenum, L.N. Næss, T.A. Peters, R. Bredesen, A. Borg, H.J. Venvik, Thickness dependent effects of solubility and surface phenomena on the hydrogen transport properties of sputtered Pd77%Ag23% thin film membranes, J. Membr. Sci. 476 (2015) 602–608, https://doi.org/10.1016/j.memsci.2014.11.031.

[21] O.M. Løvvik, Surface segregation in palladium based alloys from density-functional calculations, Surf. Sci. 583 (2005) 100–106, https://doi.org/10.1016/j.susc.2005.03.028.

[22] I.H. Svenum, J.A. Herron, M. Mavrikakis, H.J. Venvik, Adsorbate-induced segregation in a PdAg membrane model system: Pd$_3$Ag(111), Catal. Today 193 (2012) 111–119, https://doi.org/10.1016/j.cattod.2012.01.007.

[23] I.-H. Svenum, J.A. Herron, M. Mavrikakis, H.J. Venvik, Pd$_3$Ag(111) as a model system for hydrogen separation membranes: combined effects of CO adsorption and surface termination on the activation of molecular hydrogen, Top. Catal. 63 (2020) 750–761, https://doi.org/10.1007/s11244-020-01246-7.

[24] J. Greeley, M. Mavrikakis, Alloy catalysts designed from first principles, Nat. Mater. 3 (2004) 810–815, https://doi.org/10.1038/nmat1223.

[25] S. Zhu, M. Scardamaglia, J. Kundsen, R. Sankari, H. Tarawneh, R. Temperton, L. Pickworth, F. Cavalca, C. Wang, H. Tissot, J. Weissenrieder, B. Hagman, J. Gustafson, S. Kaya, F. Lindgren, I. Källquist, J. Maibach, M. Hahlin, V. Boix, T. Gallo, F. Rehman, G. D'Acunto, J. Schnadt, and A. Shavorskiy, HIPPIE: a new platform for ambient-pressure X-ray photoelectron spectroscopy at the MAX IV Laboratory, J. Synchrotron Radiat. 28 (2021) 624–636, doi:10.1107/S160057752100103X.

[26] J. Knudsen, J.N. Andersen, J. Schnadt, A versatile instrument for ambient pressure x-ray photoelectron spectroscopy: the Lund cell approach, Surf. Sci. 646 (2016) 160–169, https://doi.org/10.1016/j.susc.2015.10.038.

[27] H. Bluhm, M. Hävecker, A. Knop-Gericke, M. Kiskinova, R. Schlögl, M. Salmeron, *In situ* X-ray photoelectron spectroscopy studies of gas-solid interfaces at near-ambient conditions, MRS Bull. 32 (2007) 1022–1030, https://doi.org/10.1557/mrs2007.211.

[28] S. Doniach, M. Sunjic, Many-electron singularity in X-ray photoemission and X-ray line spectra from metals, J. Phys. C Solid State Phys. 3 (1970) 285, https://doi.org/10.1088/0022-3719/3/2/010.

[29] J.J. Yeh, I. Lindau, Atomic subshell photoionization cross sections and asymmetry parameters: 1 ⩽ Z ⩽ 103, At. Data Nucl. Data Tables. 32 (1985) 1–155, https://doi.org/10.1016/0092-640X(85)90016-6.

[30] P.J. Berlowitz, C.H.F. Peden, D.W. Goodman, Kinetics of carbon monoxide oxidation on single-crystal palladium, platinum, and iridium, J. Phys. Chem. 92 (1988) 5213–5221, https://doi.org/10.1021/j100329a030.

[31] N.M. Martin, M. Van den Bossche, H. Grönbeck, C. Hakanoglu, F. Zhang, T. Li, J. Gustafson, J.F. Weaver, E. Lundgren, CO adsorption on clean and oxidized Pd (111), J. Phys. Chem. C. 118 (2014) 1118–1128, https://doi.org/10.1021/jp410895c.

[32] H. Siegbahn, Electron spectroscopy for chemical analysis of liquids and solutions, J. Phys. Chem. 89 (1985) 897–909, https://doi.org/10.1021/j100252a005.

[33] S. Axnanda, M. Scheele, E. Crumlin, B. Mao, R. Chang, S. Rani, M. Faiz, S. Wang, A.P. Alivisatos, Z. Liu, Direct work function measurement by gas phase photoelectron spectroscopy and its application on PbS nanoparticles, Nano Lett. 13 (2013) 6176–6182, https://doi.org/10.1021/nl403524a.

[34] E.J. Crumlin, H. Bluhm, Z. Liu, *In situ* investigation of electrochemical devices using ambient pressure photoelectron spectroscopy, J. Electron Spectrosc. Relat. Phenom. 190 (2013) 84–92, https://doi.org/10.1016/j.elspec.2013.03.002.

[35] K. Christmann, G. Ertl, Adsorption of carbon monoxide on silver/palladium alloys, Surf. Sci. 33 (1972) 254–270, https://doi.org/10.1016/0039-6028(72)90208-7.

[36] L.E. Walle, H. Grönbeck, V.R. Fernandes, S. Blomberg, M.H. Farstad, K. Schulte, J. Gustafson, J.N. Andersen, E. Lundgren, A. Borg, Surface composition of clean and oxidized $Pd_{75}Ag_{25}(100)$ from photoelectron spectroscopy and density functional theory calculations, Surf. Sci. 606 (2012) 1777–1782, https://doi.org/10.1016/j.susc.2012.07.006.

[37] D. Zemlyanov, B. Aszalos-Kiss, E. Kleimenov, D. Teschner, S. Zafeiratos, M. Hävecker, A. Knop-Gericke, R. Schlögl, H. Gabasch, W. Unterberger, K. Hayek, B. Klötzer, In situ XPS study of Pd(111) oxidation. Part 1: 2D oxide formation in 10^{-3} mbar O_2, Surf. Sci. 600 (2006) 983–994, https://doi.org/10.1016/j.susc.2005.12.020.

[38] H. Gabasch, W. Unterberger, K. Hayek, B. Klötzer, E. Kleimenov, D. Teschner, S. Zafeiratos, M. Hävecker, A. Knop-Gericke, R. Schlögl, J. Han, F.H. Ribeiro, B. Aszalos-Kiss, T. Curtin, D. Zemlyanov, *In situ* XPS study of Pd(111) oxidation at elevated pressure, Part 2: palladium oxidation in the 10^{-1} mbar range, Surf. Sci. 600 (2006) 2980–2989, https://doi.org/10.1016/j.susc.2006.05.029.

[39] Y. Soma-Noto, W.M.H. Sachtler, Infrared spectra of carbon monoxide adsorbed on supported palladium and palladium-silver alloys, J. Catal. 32 (1974) 315–324, https://doi.org/10.1021/0021-9517(74)90081-5.

[40] A. Noordermeer, G.A. Kok, B.E. Nieuwenhuys, A comparative study of the behaviour of the PdAg(111) and Pd(111) surfaces towards the interaction with hydrogen and carbon monoxide, Surf. Sci. 165 (1986) 375–392, https://doi.org/10.1016/0039-6028(86)90814-9.

[41] N.A. Khan, A. Uhl, S. Shaikhutdinov, H.-J. Freund, Alumina supported model Pd–Ag catalysts: a combined STM, XPS, TPD and IRAS study, Surf. Sci. 600 (2006) 1849–1853, https://doi.org/10.1016/j.susc.2006.02.016.

[42] Y. Ma, J. Bansmann, T. Diemant, R.J. Behm, Formation, stability and CO adsorption properties of PdAg/Pd(111) surface alloys, Surf. Sci. 603 (2009) 1046–1054, https://doi.org/10.1016/j.susc.2009.02.024.

[43] Y. Ma, T. Diemant, J. Bansmann, R.J. Behm, The interaction of CO with PdAg/Pd(111) surface alloys—A case study of ensemble effects on a bimetallic surface, Phys. Chem. Chem. Phys. 13 (2011) 10741–10754, https://doi.org/10.1039/C1CP00009H.

[44] V.R. Fernandes, J. Gustafson, I.-H. Svenum, M.H. Farstad, L.E. Walle, S. Blomberg, E. Lundgren, A. Borg, Reduction behavior of oxidized Pd(100) and $Pd_{75}Ag_{25}(100)$ surfaces using CO, Surf. Sci. 621 (2014) 31–39, https://doi.org/10.1016/j.susc.2013.10.018.

[45] F. Garcia-Martinez, E. Dietze, F. Schiller, D. Gajdek, L.R. Merte, S.M. Gericke, J. Zetterberg, S. Albertin, E. Lundgren, H. Grönbeck, J.E. Ortega, Reduced carbon monoxide saturation coverage on vicinal palladium surfaces: the importance of the adsorption site, J. Phys. Chem. Lett. 12 (2021) 9508–9515, https://doi.org/10.1021/acs.jpclett.1c02639.

[46] S. Blomberg, J. Zetterberg, J. Zhou, L.R. Merte, J. Gustafson, M. Shipilin, A. Trinchero, L.A. Miccio, A. Magaña, M. Ilyn, F. Schiller, J.E. Ortega, F. Bertram, H. Grönbeck, E. Lundgren, Strain dependent light-off temperature in catalysis revealed by planar laser-induced fluorescence, ACS Catal. 7 (2017) 110–114, https://doi.org/10.1021/acscatal.6b02440.

[47] J.N. Andersen, M. Qvarford, R. Nyholm, S.L. Sorensen, C. Wigren, Surface core-level shifts as a probe of the local overlayer structure: CO on Pd(100), Phys. Rev. Lett. 67 (1991) 2822–2825, https://doi.org/10.1103/PhysRevLett.67.2822.

[48] C.J. Zhang, P. Hu, CO oxidation on Pd(100) and Pd(111): a comparative study of reaction pathways and reactivity at low and medium coverages, J. Am. Chem. Soc. 123 (2001) 1166–1172, https://doi.org/10.1021/ja002432f.

[49] A. Piednoir, M.A. Languille, L. Piccolo, A. Valcarcel, F.J. Cadete Santos. Aires, J.C. Bertolini, Pd(111) versus Pd–Au(111) in carbon monoxide oxidation under elevated pressures, Catal. Lett. 114 (2007) 110–114, https://doi.org/10.1007/s10562-007-9047-3.

[50] J. Zetterberg, S. Blomberg, J. Gustafson, J. Evertsson, J. Zhou, E.C. Adams, P.-A. Carlsson, M. Aldén, E. Lundgren, Spatially and temporally resolved gas distributions around heterogeneous catalysts using infrared planar laser-induced fluorescence, Nat. Commun. 6 (2015) 7076, https://doi.org/10.1038/ncomms8076.

[51] S. Blomberg, J. Zetterberg, J. Gustafson, J. Zhou, C. Brackmann, E. Lundgren, Comparison of AP-XPS and PLIF measurements during CO oxidation over Pd single crystals, Top. Catal. 59 (2016) 478–486, https://doi.org/10.1007/s11244-015-0524-4.

[52] B. Böller, K.M. Durner, J. Wintterlin, The active sites of a working Fischer-Tropsch catalyst revealed by operando scanning tunnelling microscopy, Nat. Catal. 2 (2019) 1027–1034, https://doi.org/10.1038/s41929-019-0360-1.

[53] T. Engel, G. Ertl, A molecular beam investigation of the catalytic oxidation of CO on Pd (111), J. Chem. Phys. 69 (1978) 1267–1281, https://doi.org/10.1063/1.436666.

[55] J. Szanyi, W.K. Kuhn, D.W. Goodman, CO oxidation on palladium. 2. A combined kinetic-infrared reflection absorption spectroscopic study of Pd (111), J. Phys. Chem. 98 (1994) 2978–2981, https://doi.org/10.1021/j100062a039.

[56] J. Wintterlin, S. Völkening, T.V.W. Janssens, T. Zambelli, G. Ertl, Atomic and macroscopic reaction rates of a surface-catalyzed reaction, Science 278 (1997) 1931–1934, https://doi.org/10.1126/science.278.5345.1931.

[57] H.-J. Freund, G. Meijer, M. Scheffler, R. Schlögl, M. Wolf, CO Oxidation as a prototypical reaction for heterogeneous processes, Angew. Chem. Int. Ed. 50 (2011) 10064–10094, https://doi.org/10.1002/anie.201101378.